Journal of the Korean Nuclear Society
Volume 12, *Number* 4, *December*, 1980

《Original》

HEXKIN: Quasistatic Approach to Spatial Kinetics Problems in a Hexagonal Lattice Reactor

Hyun Dae Kim, Se Kee Oh and Sung Ki Chae

Korea Atomic Energy Research Institute

(Received November 19, 1980)

Abstract

The quasistatic approximation is incorporated in HEXKIN, a 2-group, 2-dimensional reactor kinetics code specially developed for a hexagonal lattice-type reactor. The code allows maximum 15 delayed neutron groups, 279 lattice points, and 500 different driving functions to be able to initiate perturbation at each lattice point. Reactivity feedback due to power-dependent fuel temperature change is also involved. To check the accuracy of the code, a result of numerical experiment is compared with the measurement at the Savannah River Laboratory. The experiment was specifically designed to emphasize delayed neutron holdback. The calculated flux tilts agree with the measured flux tilts within the small uncertainty of the measurements.

요 약

Quasistatic 근사법을 이용한 2군 2차원 노심 동특성 코드 HEXKIN은 정육각형 격자 노심 계산용으로 특별히 개발되었다. 이 코드는 최대 15지발중성자군, 279격자점과 각 격자점마다 따로 입력시킬 수 있도록 500가지의 서로 다른 섭동 유도함수를 취급할 수 있다. 연료 온도 변화로 인한 반응도 궤환은 출력상태에 좌우되도록 모형화하였다. 이 코드의 정확성을 점검하기 위하여 Savannah River Laboratory에서의 측정자료로 수치실험을 수행하였다. 위의 실험은 특히 지발 중성자의 지연 효과를 강조하기 위해 계획되었다. 계산된 중성자속 틸트는 측정오차 이내에서 측정치와 잘 일치한다.

1. Introduction

This paper describes the theory and numerical experiment for testing the accuracy of the HEXKIN code[1], which employed the quasistatic method for the solution of time-dependent two-group neutron diffusion and delayed precursor equations in hexagonal geometry. The code allows maximum 15 delayed neutron groups, 279 mesh points, and 500 different driving functions to be able to initiate perturbation at each mesh point. Reactivity feedback by power-dependent fuel temperature change is also involved.

Some experiments performed in the D_2O moderated Process Development Pile (PDP)[2]

at the Savannah River Laboratory have made it possible to check the accuracy of calculation. The experiment demonstrating 'delayed neutron holdback' had very rapid reactivity insertions to a constant value which quickly caused a tilt in the flux shape. Thus, the total neutron flux shape (prompt plus delayed) did not immediately exhibit the asymptotic flux shape. The difference in the asymptotic tilt and the tilt just after the prompt jump was a direct measure of the delayed neutron holdback.

2. Numerical Experiment

2.1 HEXKIN Code

A quasistatic approximation of the time-dependent two-group neutron diffusion and delayed precursor equations in two-dimensional, hexagonal geometry is incorporated in the HEXKIN code. The method has been shown to be accurate and economic through application to the CANDU and fast reactor kinetics problems with successful results[3,4]

The quasistatic method is a flux factorization method developed to solve the time-dependent multigroup diffusion equation;

$$[-M+F_p]\phi(\vec{r},E,t)+S_d[\phi(\vec{r},E,t')] = \frac{1}{v}\frac{\partial}{\partial t}\phi(\vec{r},E,t) \quad (1)$$

where M is the removal and scattering operator, F_p the prompt fission source operator, and S_d the delayed neutron source. The total flux is partitioned with an amplitude function $N(t)$ and a shape function $\phi(\vec{r},E,t)$;

$$\phi(\vec{r},E,t)=N(t)\cdot\phi(\vec{r},E,t) \quad (2)$$

with normalized amplitude condition $N(0)=1.0$. This means the shape function $\phi(\vec{r},E,t)$ is only weakly dependent on time. The important constraint is satisfied by forcing the integral

$$\iint \frac{\phi^*(\vec{r},E,0)\phi(r,E,t)}{v}drdE \quad (3)$$

to be constant, where $\phi^*(\vec{r},E,0)$ represents the adjoint flux in steady state. Then the amplitude equation for $N(t)$ reduces to the point kinetics equation;

$$\frac{dN(t)}{dt}=\frac{[\rho(t)-\beta(t)]}{\Lambda(t)}N(t)+\sum_i\lambda_i C_i(t) \quad (4)$$

where the integral parameters $\rho(t)$, $\beta(t)$, etc. must be re-evaluated by suitable averaging with the time-dependent shape function $\phi(\vec{r},E,t.)$

Substituting the factorized total flux into the diffusion equation, the shape function takes the form:

$$[-M+F_p]\phi(\vec{r},E,t)+\frac{S_d[N(t')\cdot\phi(r,E,t')]}{N(t)} = \frac{1}{v}\left[\frac{dN}{dt}\cdot\frac{\phi(r,E,t)}{N(t)}+\frac{\partial}{\partial t}\phi(\vec{r},E,t)\right] \quad (5)$$

and the spatial precursor equations are integrated formally to obtain

$$C_i(t)=C_i(0)e^{-\lambda i t}+\int_0^t F_d{}^i\phi(\vec{r},E,t')N(t')e^{-\lambda i(t-t')}dt', i=1,2,\cdots I \quad (6)$$

here, I is defined as number of precursor groups.

A full finite difference approximation of the space and time domains is involved in the numerical method. The continuous time domain is subdivided into three different scales of time intervals; the largest, Δt_B for new shape function calculation; the medium, Δt_n for recalculating coefficients of amplitude function equation; and the smallest, Δt_k for integration of the amplitude function equation.

Reactivity feedback due to fuel temperature change with reactor power increase is involved in time-dependent reactivity estim-

ation. A simple adiabatic fuel temperature routine calculates a relative temperature difference, not actual absolute value of temperature itself, from the average power density in the core at time t:

$$P(t)=\frac{g}{V}\int\sum_{i=1}^{2}\Sigma_{fi}\Psi_i(\vec{r},t)\,d\vec{r} \qquad (7)$$

where g is the reduction factor to account for transverse power shape, V is the core volume and summation takes over neutron energy groups. After converting power change into energy variation, the average fuel temperature change is,

$$\Delta T=\frac{H_f}{F_f}\Delta E_{avg}(\Delta t_n) \qquad (8)$$

where

H_f : heat capacity of fuel

F_f : average volume fraction of fuel in a lattice cell.

$\Delta E_{avg}(\Delta t_n)$: average energy variation during time interval Δt_n

HEXKIN expresses an amount of the fuel temperature feedback effects as a change in the thermal absorption cross section of the core.

The driving function system in HEXKIN makes it possible to simulate two types of physical changes; namely, initiating mechanisms such as control movement and response mechanism such as trip actuated by period signal reaching the trip set point. In addition, changes in internal quantities due to internal conditions can be simulated, e.g., coolant density change equivalent to loss of coolant in some channels; irradiation sample extraction; clad rupture, etc. HEXKIN can treat maximum 500 different driving functions in a transient calculation, which may or may not be interrelated to one another.

2.2 Descriptions of the Measurement

The lattice used in the experiment was made up of typical Savannah River Reactor fuel and control assemblies as shown in Figure 1.

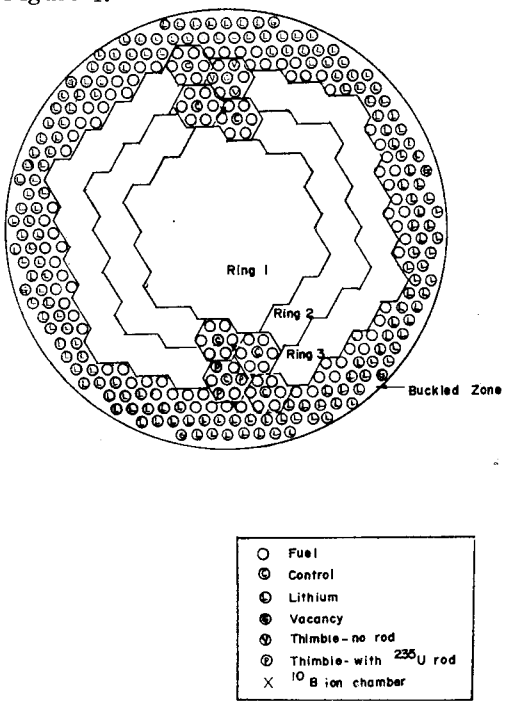

Fig. 1. Geometry of PDP

Standard supercell consists of 6 equidistance fuel sites with a control assembly in their center. All components were at a uniform 17.78cm center-to-center triangular spacing. The core is divided into 5 regions principally depending on the compositions: Ring 1, 2 and 3 composed with standard supercells; a ring of fuel-bearing assemblies for reactivity compensation; the outer 'buckled zone' containing a thin ring of lithium-bearing assemblies to minimize radial reflector effects.

To maximize the flux tilt, a location in Ring 3 was chosen as the perturbation site. However, to keep the unperturbed flux shape symmetric along the radial axis, an opposite site in Ring 3 was filled with

Table 1. Critical Water Height and Vertical Buckling Measured.

	Critical Water Height(cm)	Buckling, B_z^2 ($10^{-6}cm^{-2}$)	Buckling, ΔB_z^2 ($10^{-6}cm^{-2}$)
Base lattice	247.70±0.02	246.6±1.3	—
Perturbation and dummy sites installed			
Unperturbed	247.95±0.02	246.0±1.3	−0.62±0.05
Perturbed	244.96±0.02	253.5±1.3	+6.89±0.05

dummy elements as if to receive the perturbation. Ion chambers were located at different radial positions along this diagonal but identical axial level were used to monitor the transient flux profile. Flux tilt was measured by pairs of symmetrically placed ion chambers and was defined as:

$$[\phi(t)/\phi(0)]A/[\phi(t)/\phi(0)]B$$

where A and B refer to ion chamber locations.

The reactivity transients were initiated by dropping three ^{235}U-bearing rods into the lattice at the perturbation site. For each rod drop position and its symmetric counterpart, a fuel rod was removed and replaced with an air-filled thimble. The reactivity insertion constituted essentially a linear ramp of 0.274-sec duration.

Static reactivity measurements for perturbation rods, dummy sites, and detector thimbles were made against critical moderator height. The measured values are listed in Table 1 to give essential information to normalize the simulation model.

2.3 Simulation of the Experiment

As HEXKIN allows maximum 279 mesh points, the reactor described in the previous section was rearranged to adapt the coarse mesh model. The choice of 4 lattices as one mesh was applied for the simulation and is illustrated in Figure 2.

In practice, homogenization of the material compositions over a quite large mesh area and calculation of the pointwise detector

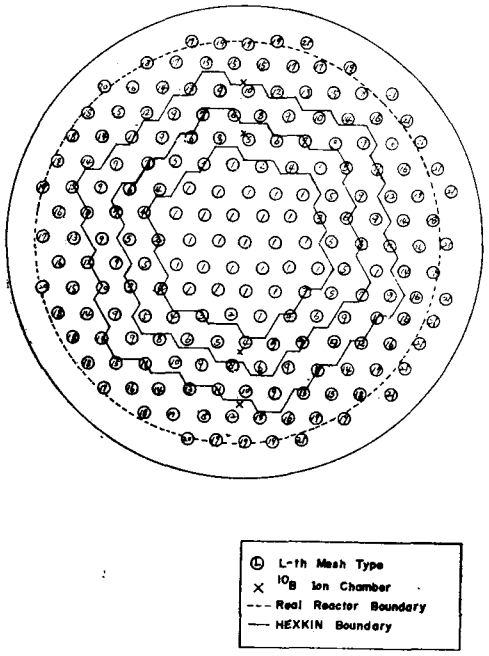

Fig. 2. HEXKIN Model

response from mesh-averaged flux were found to result in a small ambiguity in the interpretation of the calculated tilts.

Two-group cross sections evaluated over the supercell were used in the control zone (Ring 1, 2 and 3). Cross sections in a mesh consisted of different Ring's fuel sites were factorized by their volume fractions in the mesh. Table 2 gives unnormalized macroscopic 2-group cross-sections and neutron velocities for the experiment. Also the delayed neutron precursor group structure effective over the whole reactor is given in Table 3.

At the first stage, a static eigenvalue

Table 2. Unnormalized Two Group Cross Sections and Velocities for HEXKIN Model.

Mesh Type	Group	D(cm)	Σ_a(cm^{-1})	$\nu\Sigma_f$(cm^{-1})	Σ_r(cm^{-1})	$\frac{1}{v}$(sec/cm)	χ
1	1	1.38250	0.349074×10^{-2}	0.226216×10^{-2}	0.816457×10^{-2}	0.89414×10^{-7}	1.0
	2	0.897522	0.315775×10^{-1}	0.230623×10^{-1}	—	0.31724×10^{-5}	0.0
2	1	1.38251	0.348958×10^{-2}	0.225350×10^{-2}	0.817938×10^{-2}	0.89547×10^{-7}	1.0
	2	0.897514	0.315589×10^{-1}	0.229690×10^{-1}	—	0.31724×10^{-5}	0.0
3	1	1.38253	0.348842×10^{-2}	0.224483×10^{-2}	0.819418×10^{-2}	0.89680×10^{-7}	1.0
	2	0.897506	0.315402×10^{-1}	0.228736×10^{-1}	—	0.31725×10^{-5}	0.0
4	1	1.38254	0.348725×10^{-2}	0.223616×10^{-2}	0.820898×10^{-2}	0.89812×10^{-7}	1.0
	2	0.897498	0.315215×10^{-1}	0.227732×10^{-1}	—	0.31735×10^{-5}	0.0
5	1	1.38255	0.348609×10^{-2}	0.222750×10^{-2}	0.822378×10^{-2}	0.89945×10^{-7}	1.0
	2	0.897490	0.315028×10^{-1}	0.226848×10^{-1}	—	0.31726×10^{-5}	0.0
6	1	1.38052	0.337323×10^{-2}	0.220633×10^{-2}	0.818987×10^{-2}	0.89197×10^{-7}	1.0
	2	0.895209	0.299166×10^{-1}	0.221358×10^{-1}	—	0.32193×10^{-5}	0.0
7	1	1.37849	0.326038×10^{-2}	0.218516×10^{-2}	0.815597×10^{-2}	0.88450×10^{-7}	1.0
	2	0.892929	0.283304×10^{-1}	0.215868×10^{-1}	—	0.32661×10^{-5}	0.0
8	1	1.37645	0.314753×10^{-2}	0.216398×10^{-2}	0.812206×10^{-2}	0.87702×10^{-7}	1.0
	2	0.890648	0.267441×10^{-1}	0.210377×10^{-1}	—	0.33128×10^{-5}	0.0
9	1	1.37442	0.303467×10^{-2}	0.214281×10^{-2}	0.808816×10^{-2}	0.86954×10^{-7}	1.0
	2	0.888368	0.251579×10^{-1}	0.204887×10^{-1}	—	0.33596×10^{-5}	0.0
10	1	1.37717	0.312649×10^{-2}	0.220578×10^{-2}	0.800754×10^{-2}	0.86650×10^{-7}	1.0
	2	0.892194	0.270288×10^{-1}	0.220218×10^{-1}	—	0.33053×10^{-5}	0.0
11	1	1.37991	0.321832×10^{-2}	0.226875×10^{-2}	0.792692×10^{-2}	0.86345×10^{-7}	1.0
	2	0.896020	0.288995×10^{-1}	0.235549×10^{-1}	—	0.32510×10^{-5}	0.0
12	1	1.38065	0.331013×10^{-2}	0.233172×10^{-2}	0.784630×10^{-2}	0.86040×10^{-7}	1.0
	2	0.899846	0.307703×10^{-1}	0.250880×10^{-1}	—	0.31967×10^{-5}	0.0
13	1	1.38139	0.340195×10^{-2}	0.239469×10^{-2}	0.776568×10^{-2}	0.85736×10^{-7}	1.0
	2	0.903671	0.326411×10^{-1}	0.266211×10^{-1}	—	0.31423×10^{-5}	0.0
14	1	1.36254	0.262003×10^{-2}	0.179602×10^{-2}	0.859788×10^{-2}	0.90010×10^{-7}	1.0
	2	0.887067	0.255065×10^{-1}	0.199658×10^{-1}	—	0.33570×10^{-5}	0.0
15	1	1.34369	0.183818×10^{-2}	0.119735×10^{-2}	0.943009×10^{-2}	0.94283×10^{-7}	1.0
	2	0.870464	0.183719×10^{-1}	0.133106×10^{-1}	—	0.35718×10^{-5}	0.0
16	1	1.32484	0.105620×10^{-2}	0.598675×10^{-3}	0.102623×10^{-1}	0.98557×10^{-7}	1.0
	2	0.853860	0.112372×10^{-1}	0.665530×10^{-2}	—	0.37865×10^{-5}	0.0
17	1	1.30599	0.274282×10^{-3}	0.0	0.110945×10^{-1}	0.10283×10^{-6}	0.0
	2	0.837256	0.410254×10^{-2}	0.0	—	0.40012×10^{-5}	0.0
18	1	1.24577	0.669461×10^{-3}	0.0	0.148704×10^{-1}	0.10200×10^{-6}	0.0
	2	0.708650	0.113919×10^{-1}	0.0	—	0.38802×10^{-5}	0.0
19	1	1.18555	0.106464×10^{-3}	0.0	0.186463×10^{-1}	0.10116×10^{-6}	0.0
	2	0.580043	0.186813×10^{-1}	0.0	—	0.37593×10^{-5}	0.0
20	1	1.12533	0.145982×10^{-2}	0.0	0.224221×10^{-1}	0.10032×10^{-6}	0.0
	2	0.451437	0.259706×10^{-1}	0.0	—	0.36383×10^{-5}	0.0
21	1	1.06510	0.185500×10^{-2}	0.0	0.261980×10^{-1}	0.99488×10^{-7}	0.0
	2	0.322830	0.332600×10^{-1}	0.0	—	0.35173×10^{-5}	0.0

calculation is to compute the critical moderator height compared with the measured dimension. In general, the eigenvalues calculated will differ from unity due to uncertainties in cross sections and truncation errors in numerical method, and require

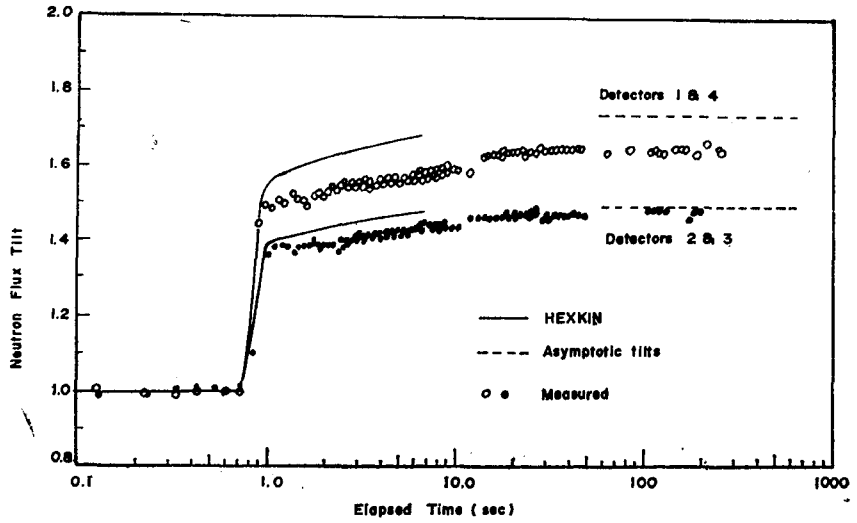

Fig. 3. Measured and Calculated Flux Tilts

some form of normalization to agree with the measured critical configurations. The normalization procedure used is to adjust only the production cross sections, $\nu\Sigma_f$.

For the reference, $\nu\Sigma_f$ is varied by the same fractional amount in all fuel-bearing meshes until calculated and measured vertical bucklings agree at critical.

The second adjustments are for the worths of the perturbation and dummy sites with and without perturbing rods. Again, cumulative composition, transport, and diffusion theory errors are effectively compensated by making necessary changes in $\nu\Sigma_f$ at these sites.

3. Results

Figure 3 shows the measured and calculated flux tilts as a function of time. Because of the long running time, HEXKIN calculations were taken up to 6.2 seconds from transient initiation. This is equivalent to only about 90% of the asymptotic flux tilt distribution which was reached before the transient was terminated.

Table 3. Effective Delayed Neutron Precursor Groups.

Group i	$\beta_i^{eff} \times 10^{-5}$	$\lambda_i(\text{sec}^{-1})$
1	16.80	3.871
2	82.57	1.400
3	309.92	0.3058
4	121.09	0.1150
5	176.57	0.02781
6	11.09	0.002598

The tilts between the detector pairs resulting from this positive reactivity insertion were calculated with small discrepancies.

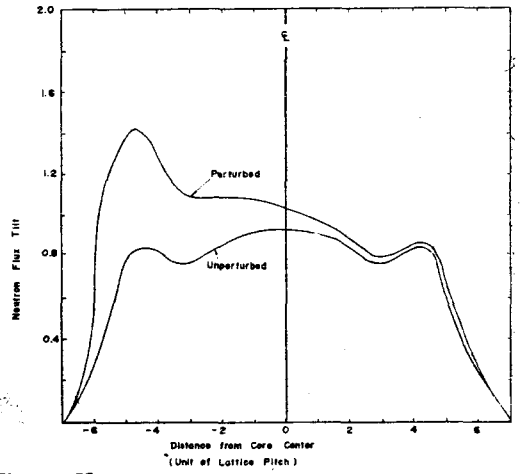

Fig. 4. Neutron Flux Shape for the Perturbed and Unperturbed Core

the absolute tilt for detector pair 1 and 4 was overestimated by 6.7%; that for 2 and 3 was overestimated by 3.8%.

The coarse mesh method contributes to uncertainties in homogenizing procedures particularly for the perturbing and dummy sites where local flux variations are severe. And to obtain exact detector response, no satisfactory method was found to compute the intramesh flux distribution for meshes in which neutron fluxes vary remarkably. Only the way to reduce errors is assuming smooth flux distribution shape along the diagonal direction and interpolating the detector response from the environmental four mesh fluxes. Figure 4 illustrates static and asymptotic flux shapes for diagonal direction passing through the nearest meshes to detector sites.

4. Conclusion

The HEXKIN code accurately predicts the transient responses of the thermal reactor, with the following qualifications:

1. Only the coarse mesh model was used in the test.

2. Only the amount and time dependence of the delayed neutron holdback in the calculation have been directly tested with a small amount of reactivity perturbation.

3. Only interstitial detector position was used in the experiment.

The transients of this experiment were calculated at very reasonable cost in terms of compting time. CPU time in CDC Cyber 73 consumed in the calculation of 6.2 seconds reactor time with trial time interval of 0.014 sec and the flux convergence criterion of 1.0×10^{-4} was about 240 seconds.

References

1) H.D. Kim, S.K. Oh and S.K.. Chae, HEXKIN: A Fortran Ⅳ Program to Solve 2-Dimensional Reactor Kinetics Problem in the Hexagonal Geometry, Part 1, User's Manual and Program Description, KAERI-RDP/300-A34-2, 1980.

2) Albert E. Dunklee, The Heavy Water System of the Process Development Pile, DP-567, 1961.

3) G. Kugler and A.R. Dastur, Accuracy of the Improved Quasistatic Space-time Method Checked with Experiment, AECL-5553, 1976.

4) A.R. Dastur and D.B. Buss, Space-time Kinetics of CANDU Systems, Proc. NEACRP/CSNI Specialists Meeting on 'New Developments in 3-D Neutron Kinetics and Review of Benchmark Calculations', München, 1975.

5) P.B. Parks, N.P. Baumann, R.L. Currie and C.E. Jewell, Multidimensional Space-time Nuclear-reactor Kinetics Studies - Part Ⅱ: Experimental, *Nucl. Sci. Eng.*, **59**, 298-310, 1976.